Error Budget in $\pi^+ \rightarrow e^+ \nu$ Experiment

April 4, 2006

1 $\pi^+ \rightarrow e^+ \nu$ Lineshape

1.1 Simulation of the Photonuclear and Electronuclear Reactions: the current PIBETA simulation

The current PIBETA detector Monte Carlo Simulation is written in FOR-TRAN using GEANT3 subroutines. The latest GEANT version 3.21 does not take into account interactions of photons and electrons/positrons with nuclei. In our simulation we have added the Giant Dipole Resonance (GDR) cross sections for the photons in the energy range 10–100 MeV in a separate user routine. The relevant technical note provides the implementation details [1].

Using extended GEANT3 code we have compared the detector response to the $\pi^+ \rightarrow e^+ \nu$ events with and without GDR reactions. We find that in $0.88 \pm 0.03,\%$ of the events photon undergoes the photonuclear absorption. Assuming that the photonuclear reaction completely removes the absorbed photon energy from the shower, we find that the positron lineshape tail below ~ 50 MeV is increased by 10 %.

The full Monte Carlo simulation of the $\pi^+ \rightarrow e^+ \nu(\gamma)$ lineshape that includes the radiative corrections was smoothed using the neural network with 4 hidden neurons in 3-layer percepton. The $\pi^+ \rightarrow e^+ \nu$ tail fraction (for the default PIBETA $\pi^+ \rightarrow e^+ \nu$ software cuts) is 2.15 % for 52 MeV high-level energy threshold, 1.50 % for 51 MeV, 1.20 % for 50 MeV, 0.90,% for 49 MeV and 0.75 % for 48 MeV. These tail fractions, for the present calculation, have

1

about 10 % systematic uncertainty. The dependence of the lineshape tail fraction on the value of the high energy threshold is shown in Fig. 1.

For Michel positrons the simulation predicts that the corresponding fraction of photoabsorbed photons is 0.43±0.02. The quoted errors are statistical uncertainties.

1.2   Simulation of the Photonuclear and Electronuclear Reactions: GEANT4 Monte Carlo

GEANT4 includes the parameterization of photonuclear and electronuclear cross sections in two energy regions relevant for our experiment [2]:

- the Giant Dipole Resonance (GDR) region, depending on the nucleus, extends from 10 MeV up to 30 MeV. It usually consists of one large peak, though for some nuclei several peaks appear.

- the "quasi-deuteron" region extends from around 30 MeV up to the pion threshold and is characterized by small cross sections and a broad, low peak.

In the GEANT4 photonuclear database there are about 50 nuclei for which the photonuclear absorption cross sections have been measured in the above energy ranges. These experimental data points are used to parameterize the photonuclear absorption cross sections.

Electronuclear reactions are so closely connected with photonuclear reactions that they are sometimes called "photonuclear" because the one-photon exchange mechanism dominates in electronuclear reactions. In this sense electrons can be replaced by a flux of equivalent photons. For our energy range, below 70 MeV, this is an excellent description [3, 4].

We should write a "toy-model" of the PIBETA detector in GEANT4 and study the effects of the photo/electronuclear reactions on the $\pi^+ \rightarrow e^+\nu$ and Michel e^+'s lineshapes.

2   Hadronic interactions of the π^+ Beam

2.1   The GEANT3 Monte Carlo simulation for $67 < p_{\pi^+} < 115\,\mathrm{MeV}$

We have used the GEANT3 Monte Carlo with GEISHA/FLUKA hadronic packages to model the frequency of the inelastic hadronic interactions of the positive pion beam in the plastic scintillator. The incident momentum range of the π^+ beam was between $115\,\mathrm{MeV}$ to $67\,\mathrm{MeV}$. The calculation predicts the prompt interactions in the detectors (degrader plus active target) to decrease from $\sim 0.1\,\%$ to $< 0.01\,\%$. This fall-off is shown in Fig. 16.

3   Determination of the time scale: effects of uncertainties in zero time offset

We have directly coded the time dependences of the $\pi^+ \to e^+\nu$ and $\mu^+ \to e^+\nu\nu$ decay in FORTRAN. In Fig. 17 we show how the uncertainty in the zero time point affects the extracted ratio of branching ratios. In order to measure the $\mathrm{BR}(\pi^+ \to e^+\nu)/\mathrm{BR}(\mu^+ \to e^+\nu\nu)$ with $5 \cdot 10^{-4}$, the absolute zero of the time scale has to be measured with the precision of $0.007\,\mathrm{ns}$.

References

[1] E. Frlež, Photonuclear Reactions in `GEANT` Code (1995), accessible at URL `http://helena.phys.virginia.edu/~ pibeta/`.

[2] H. P. Wellisch and D. H. Wright, in *GEANT4 Physics Reference Manual* (2004), accessible at URL `http://geant4.web.cern.ch`.

[3] I. Ya. Pomeranchuk and I. M. Shmushkevich, Nucl. Phys. 23, 1295 (1961).

[4] V.N. Gribov et al., ZhETF 41, 1834 (1961).
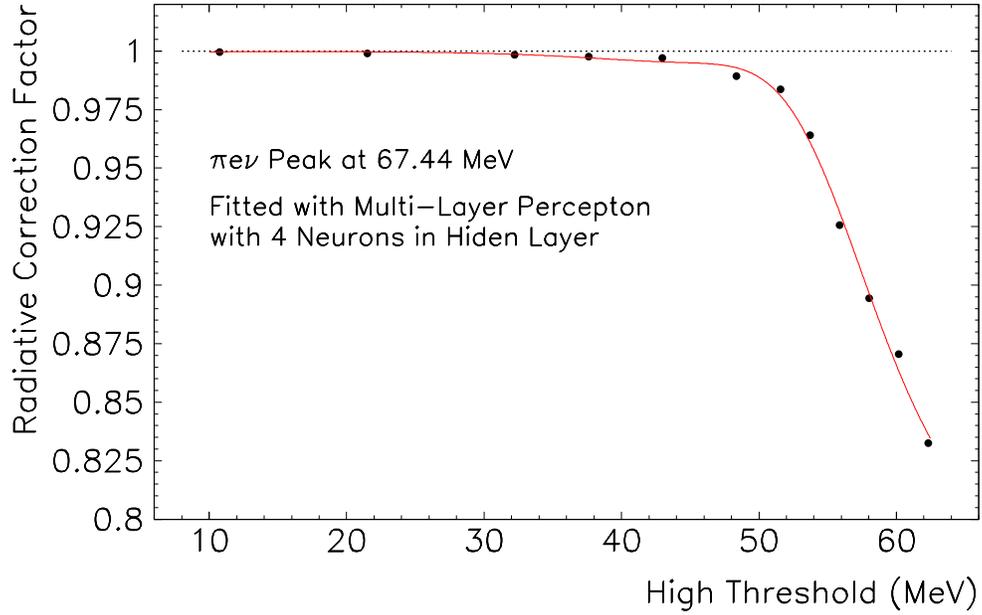
Figure 1: GEANT3 Monte Carlo simulation of the PIBETA detector. The full radiative pion decay $\pi^+ \rightarrow e^+\nu$ was simulated in high-statistics run. The smoothing was done using the neural network with 4 hiden neurons in 3-layer percepton. The $\pi^+ \rightarrow e^+\nu$ tail fraction for $52\,\mathrm{MeV}$ high-level energy threshold is $2.15\,\%$.
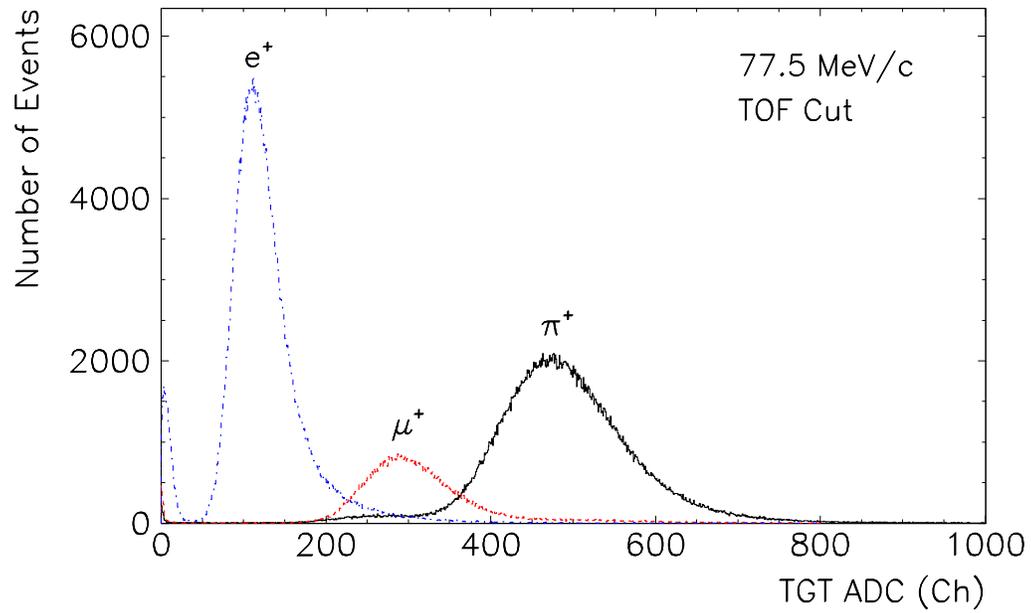
Figure 2: Target energy spectra for 77.25 MeV/c beam. The forward beam counter was 5 mm thick plastic scintillator. The target was 15 mm thick plastic scintillator. Particle identification was done by time-of-flight method.
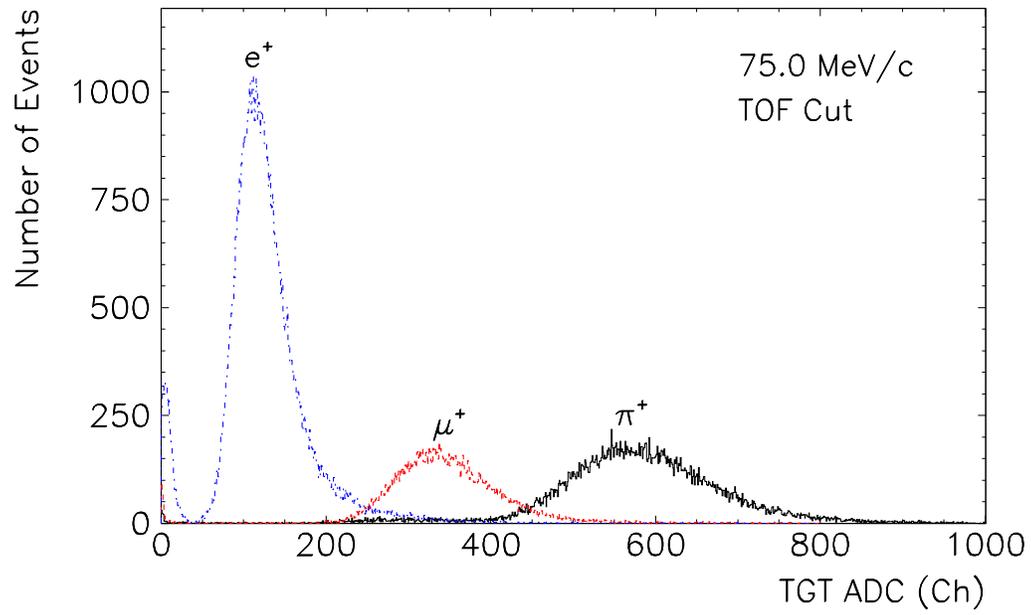
Figure 3: Target energy spectra for $75.0\,\mathrm{MeV/c}$ beam.
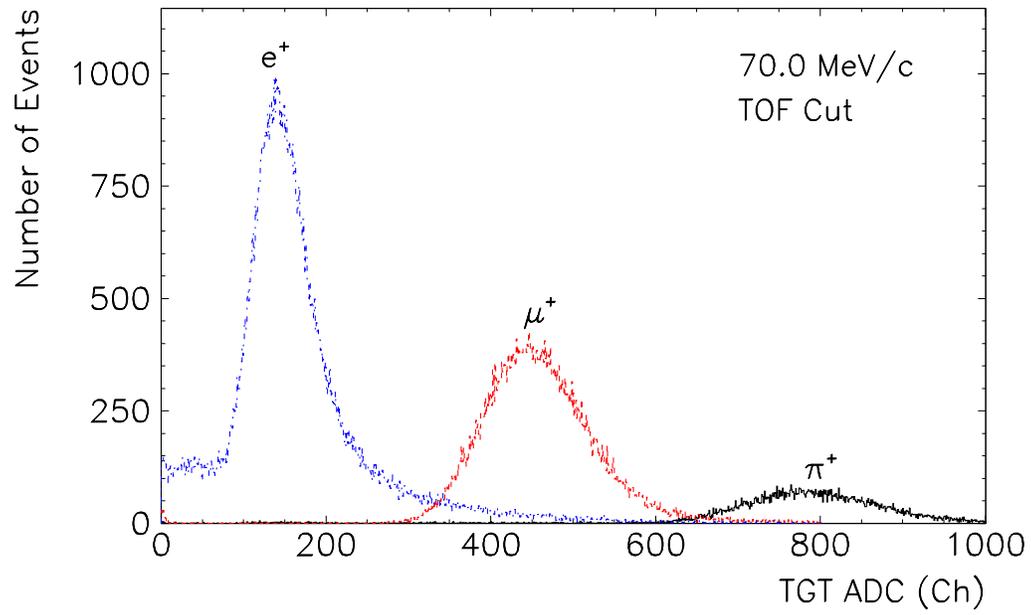
Figure 4: Target energy spectra for $70.0\,\mathrm{MeV/c}$ beam.
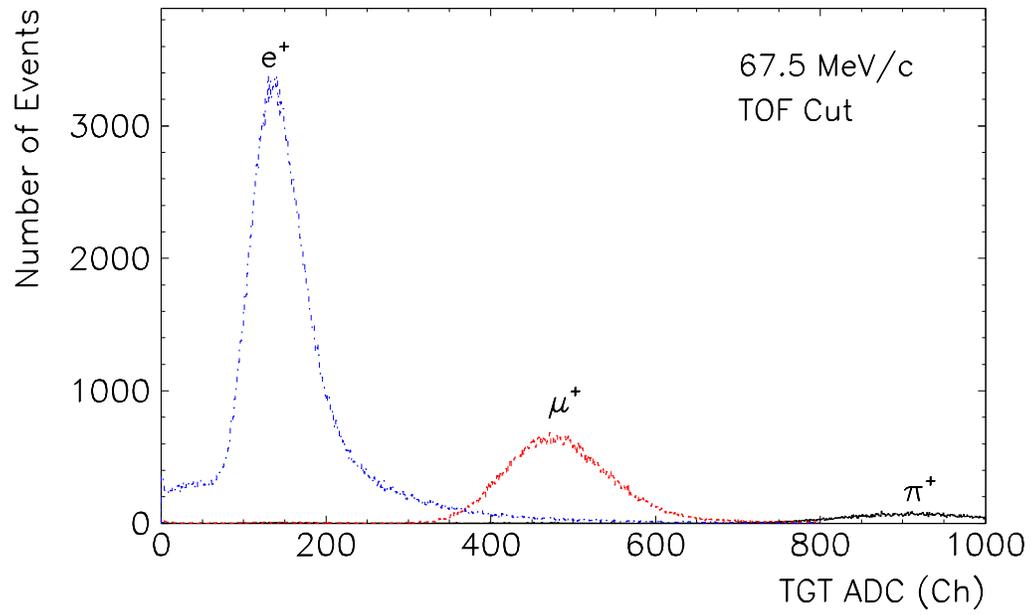
Figure 5: Target energy spectra for $67.50\,\mathrm{MeV/c}$ beam.
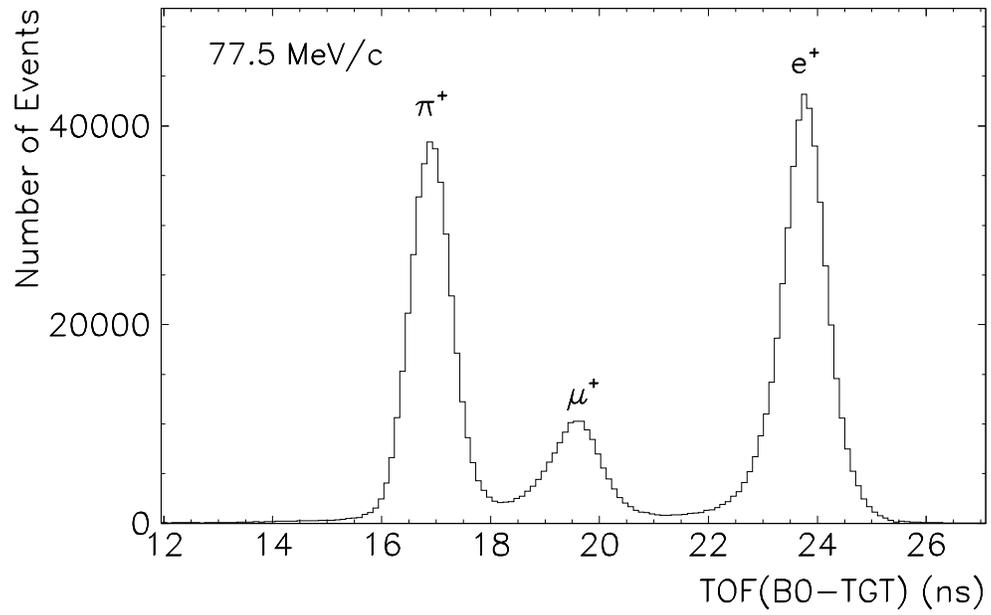
Figure 6: The beam particle time-of-flight for 77.25 MeV/c beam momentum.
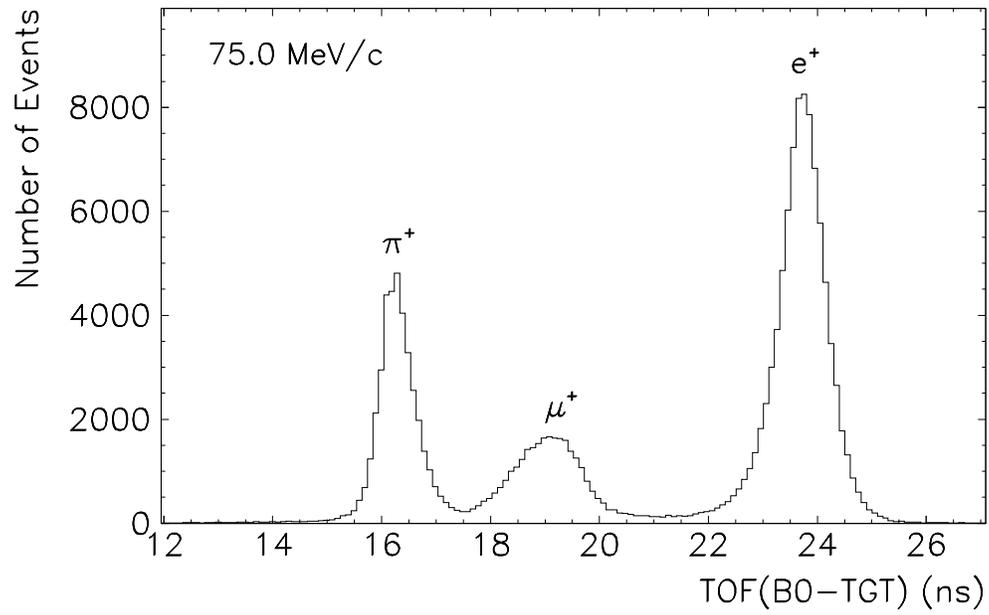
Figure 7: The beam particle time-of-flight for 75.0 MeV/c beam momentum.
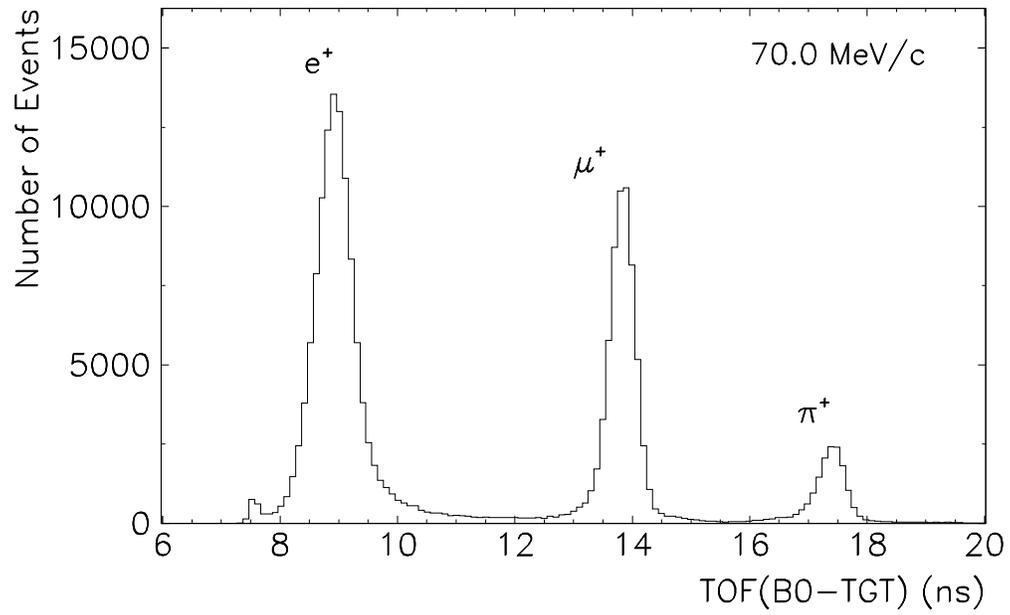
Figure 8: The beam particle time-of-flight for 70.0 MeV/c beam momentum.
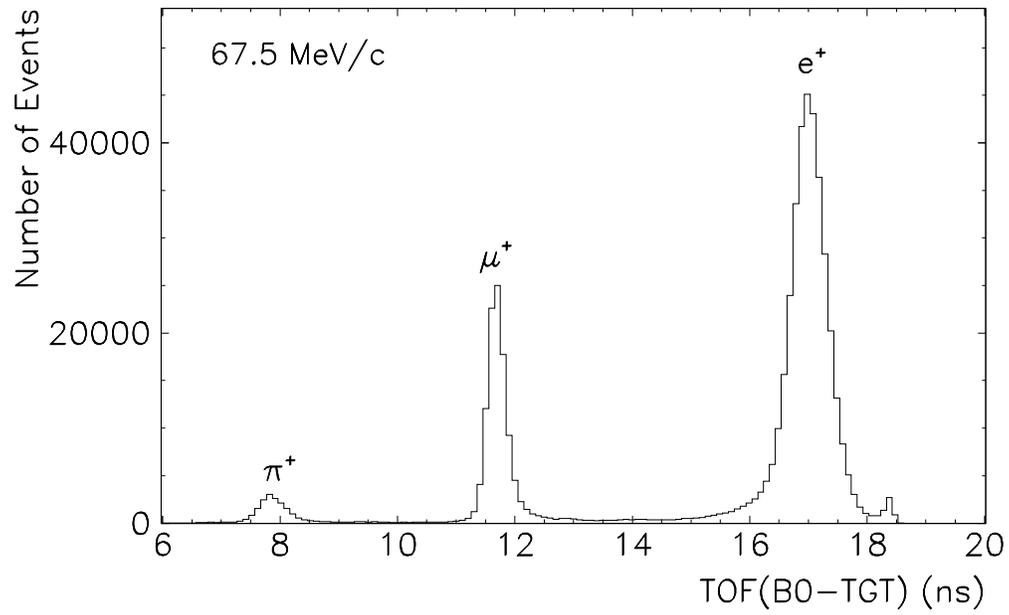
Figure 9: The beam particle time-of-flight for $67.5\,\mathrm{MeV/c}$ beam momentum.
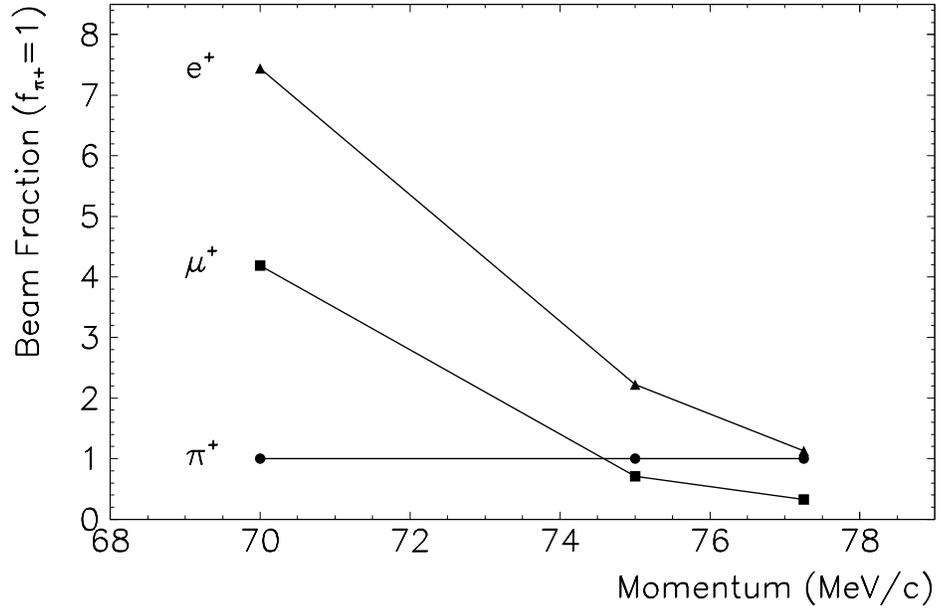
Figure 10: π^+, μ^+ and e^+ beam fractions for beam momentum interval 77.25–70.0 MeV/c. The particle ID was done by fitting the time-of-flight spectra.
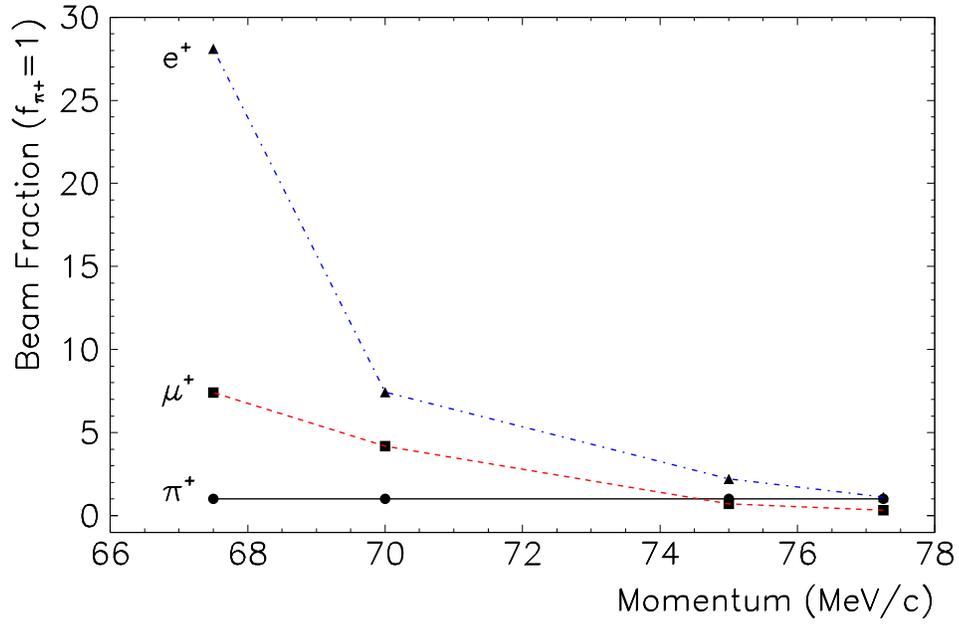
Figure 11: π^+, μ^+ and e^+ beam fractions for beam momentum interval 77.25–67.5 MeV/c. The particle ID was done by fitting the time-of-flight spectra. μ^+ and e^+ fractions are normalized to π^+ flux.
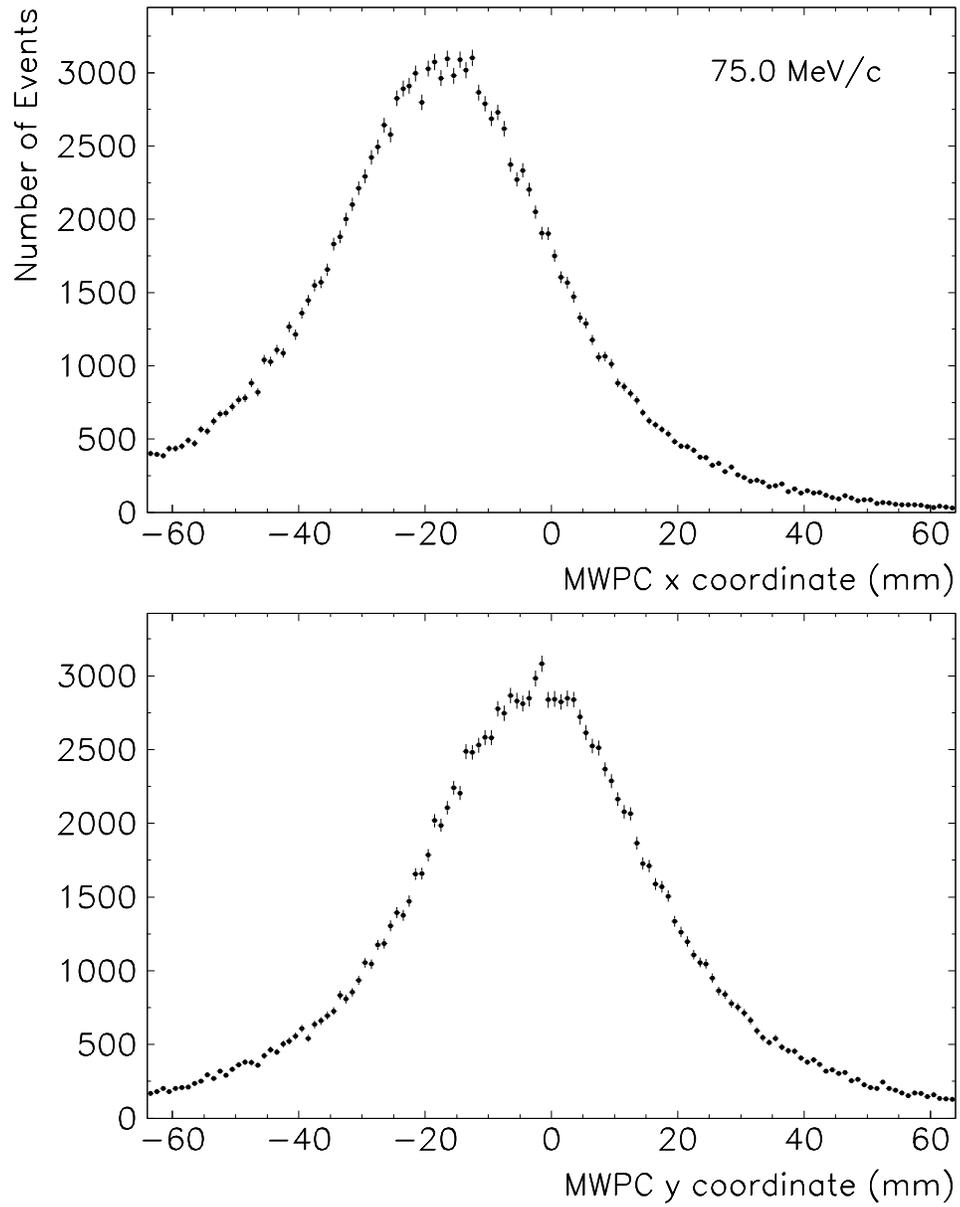
Figure 12: Horizontal (top) and vertical (bottom) beam profiles at the "target" position for 75 MeV/c beam. Tracking was done with two $130\times130\,\mathrm{mm}^2$ MWPCs.
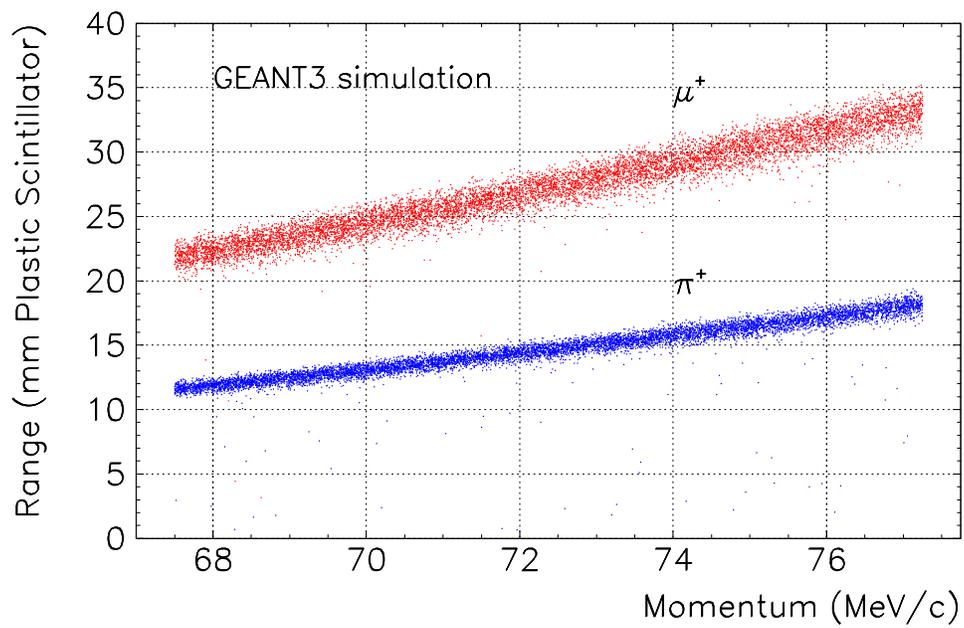
Figure 13: GEANT3 simulation of π^+ and μ^+ beam particles' stopping range in the plastic scintillator. 10^4 events were generated in momentum range 67.5–77.25 MeV/c with the measured x, y beam divergence.
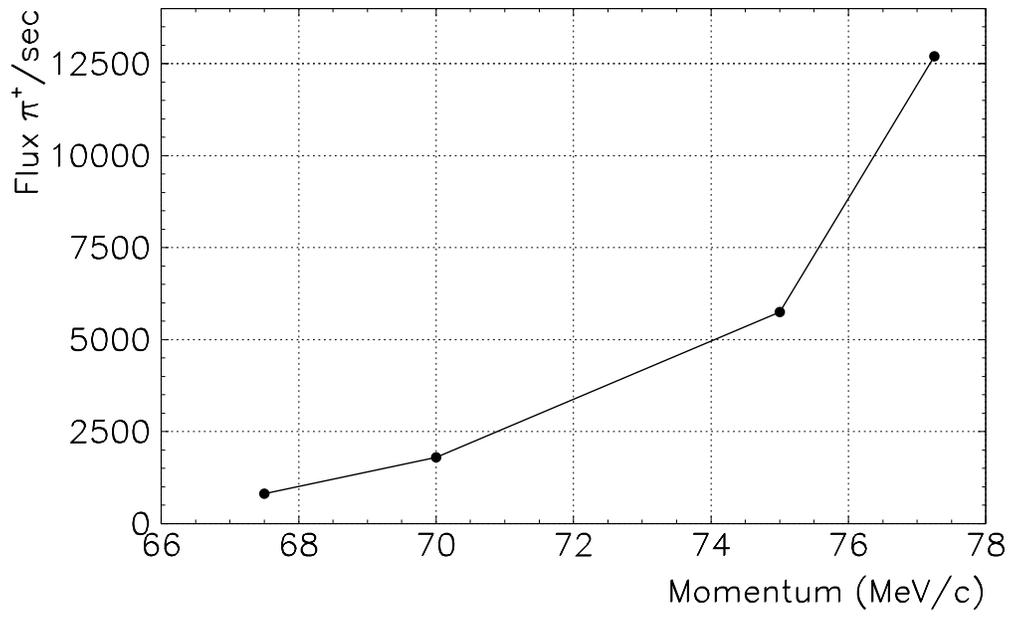
Figure 14: Four new beam tunes: π^+ intensity at ca. one meter from collimator in the momentum range 67.5–77.25 MeV/c.
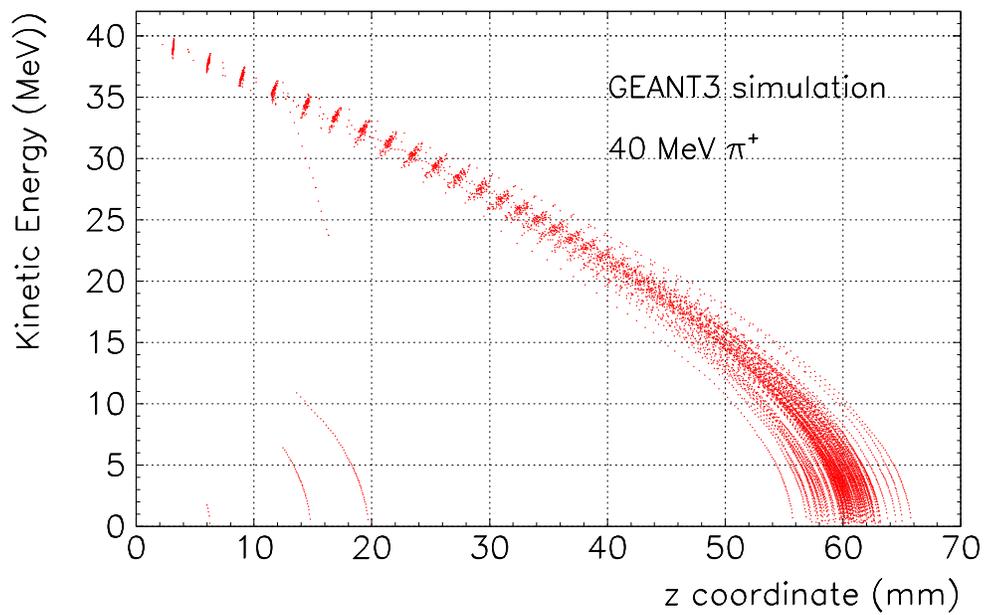
Figure 15: Positive pion beam stopping in the plastic scintillator: the GEANT3 calculation shows the relationship between the pion pathlength in cm and its kinetic energy in MeV.
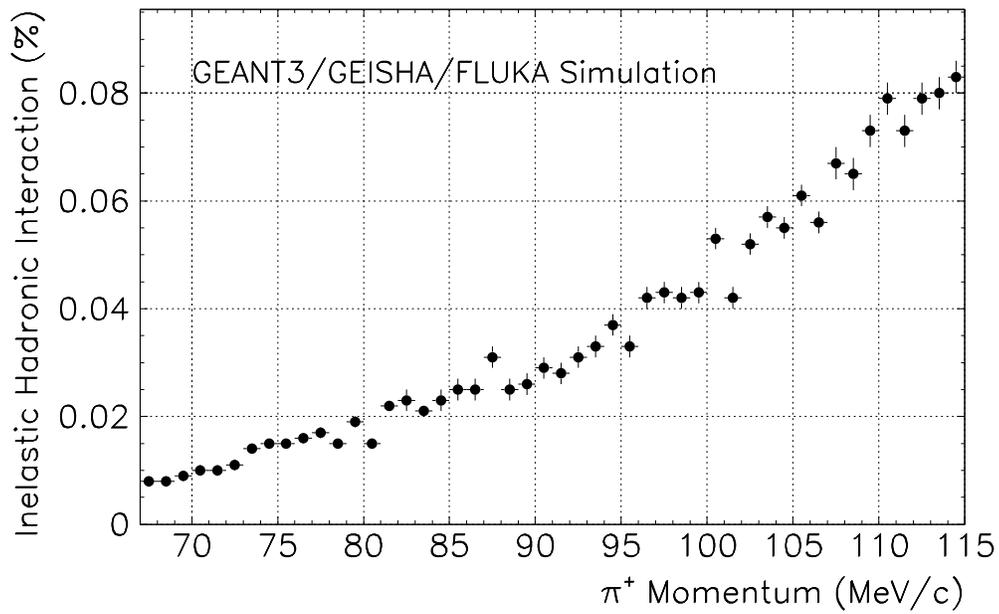
Figure 16: Fall-off of inelastic hadronic interactions of the π^+ beam in the plastic scintillator from $115\,\text{MeV}$ to $67\,\text{MeV}$: the GEANT3 calculation with GEISHA/FLUKA hadronic packages predicts the prompt interactions to decrease from $0.1\,\%$ to $< 0.01\,\%$.
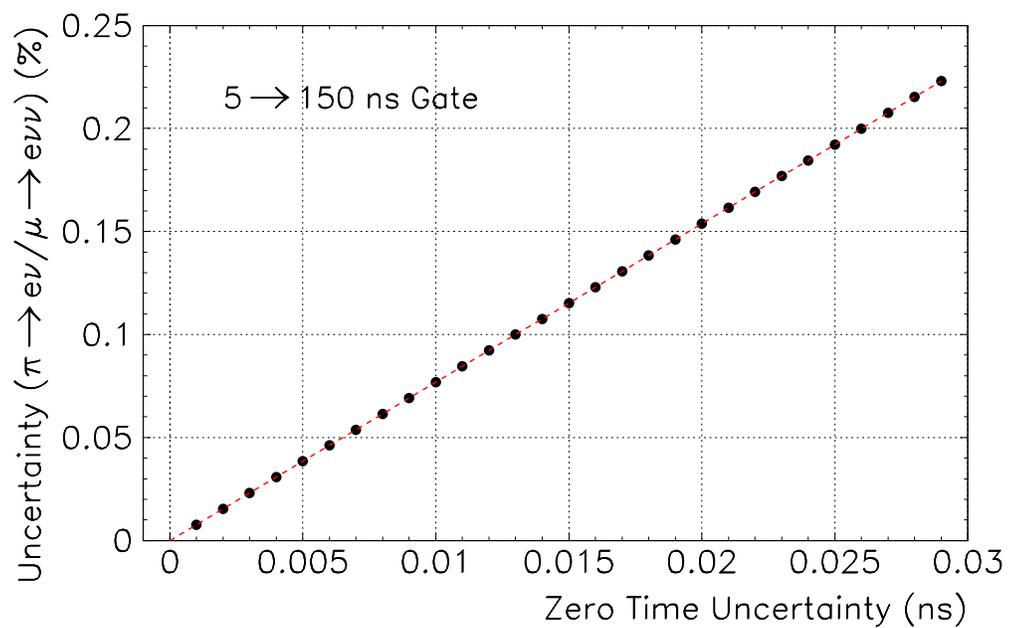
Figure 17: Dependence of the uncertainty of the ratio $\mathrm{BR}(\pi^+ \rightarrow e^+\nu(\gamma))/\mathrm{BR}(\mu^+\nu\nu)$ on the zero time uncertainty.
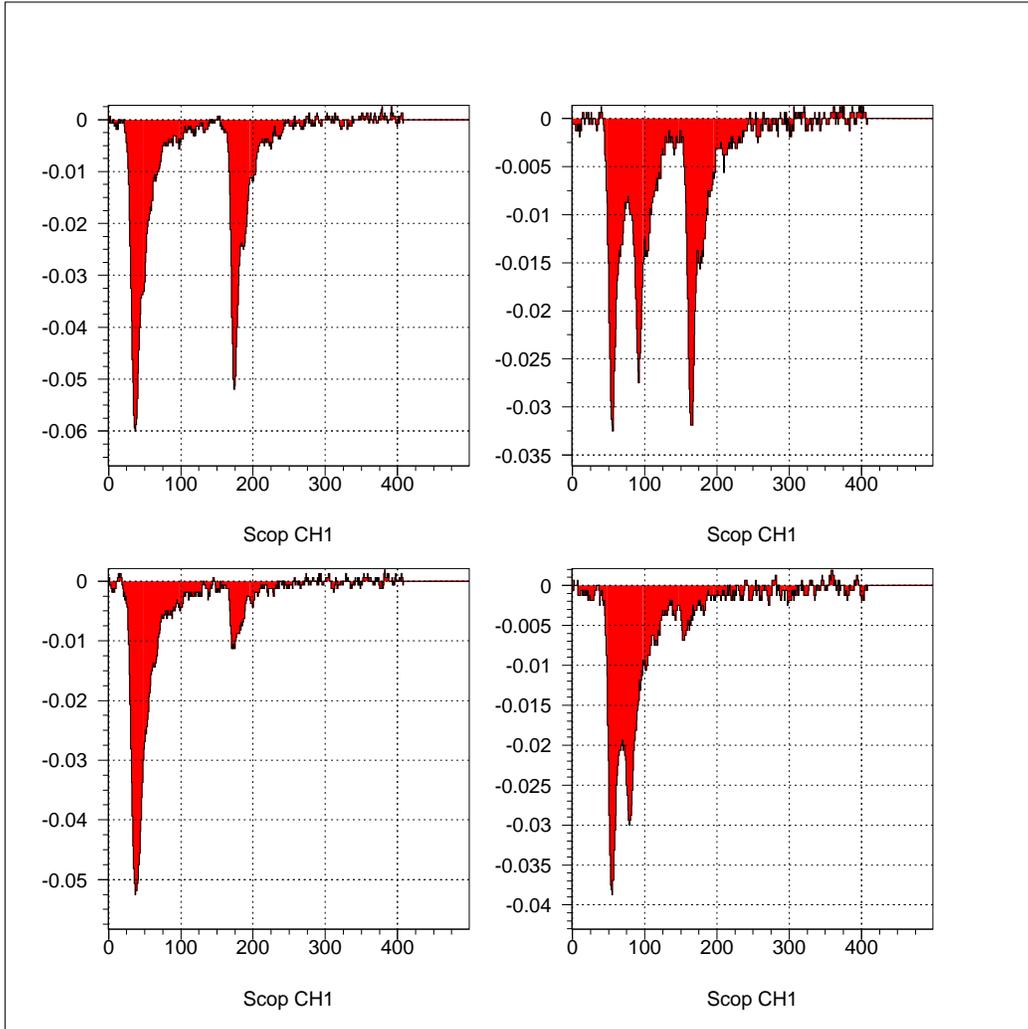
Figure 18: Oscilloscope-captured waveforms of the $\mu^+ \rightarrow e^+ \nu\nu$ decays. The time scale is 5 channels/ns. The target was fast scintillator viewed with the 2 inch PMT.
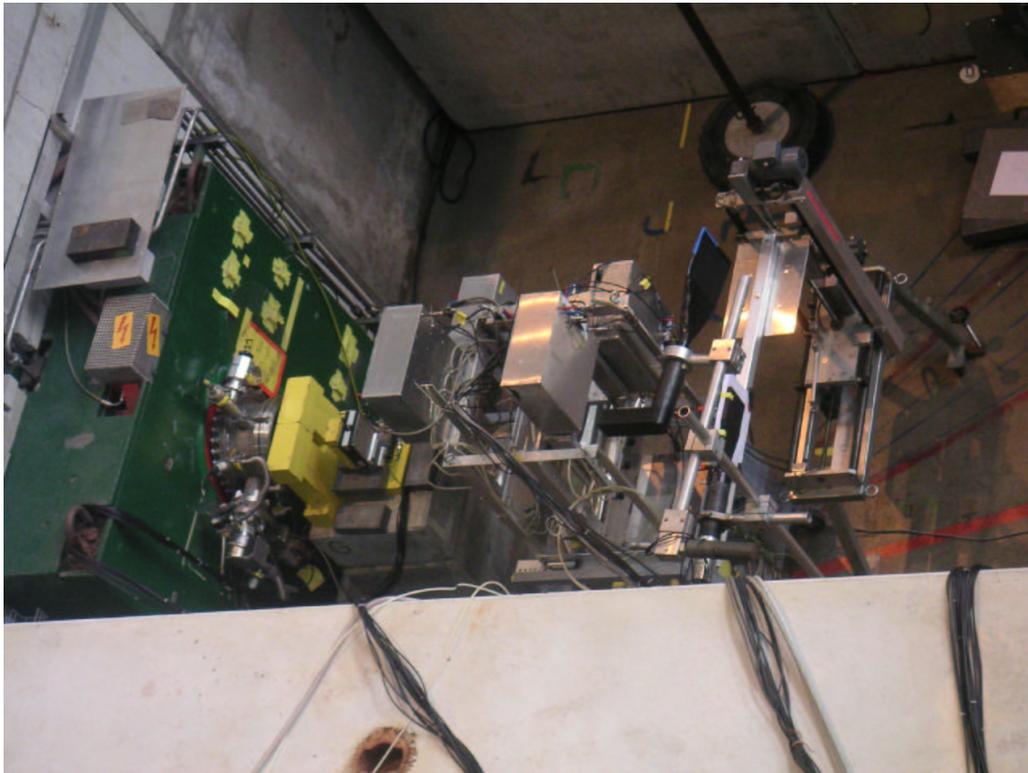
Figure 19: The layout of the PSI πE1 experimental area for beam-definition studies. The lead collimator (yellow) and two plastic beam counters can be seen.
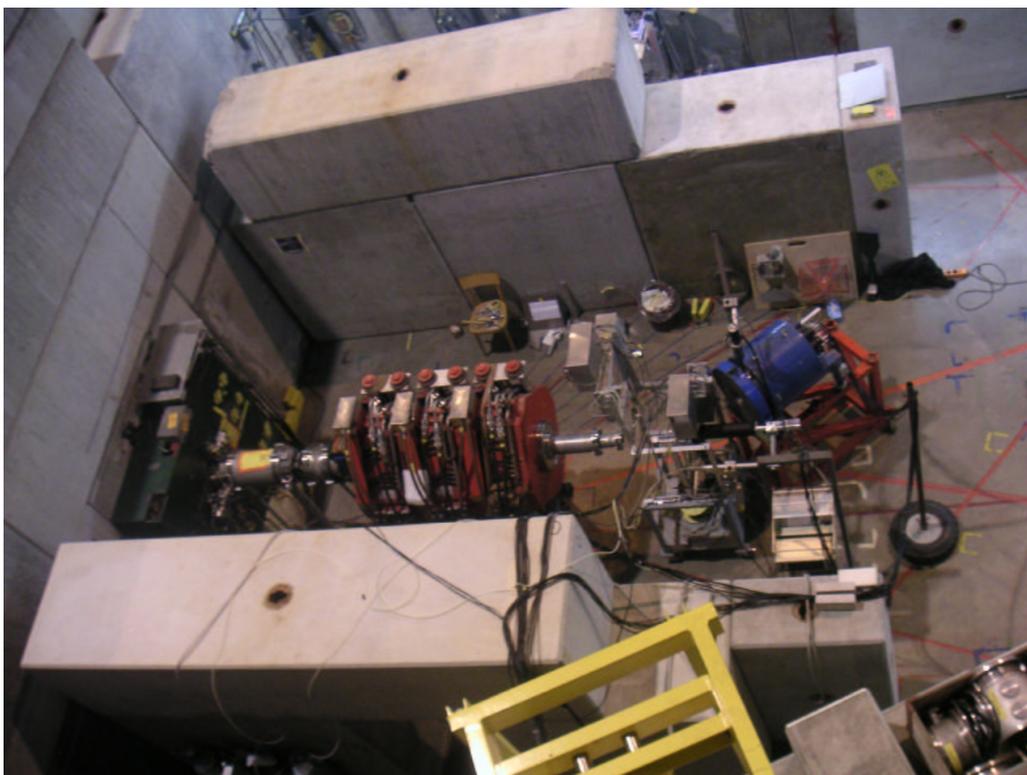
Figure 20: The layout of the PSI πE1 experimental area for $\pi^+ \rightarrow e^+\nu$ measurement. The NaI calorimeter can be seen at the right.